Hydrogen-induced defects in ion-implanted Si

S. Socher,* E. V. Lavrov, and J. Weber
Technische Universität Dresden, 01062 Dresden, Germany
(Received 4 July 2012; published 20 September 2012)

Single crystalline silicon implanted with ^{28}Si ions and subsequently hydrogenated from an rf plasma at 200 °C is studied by Raman and photoluminescence spectroscopy. A broad Raman band at 3830 cm^{-1} previously assigned to the rovibrational transitions of hydrogen molecules trapped in Si multivacancies [Ishioka *et al.*, Phys. Rev. B **60**, 10852 (1999)] reveals a complex line shape at 60 K. In contrast, our study correlates the Raman band to three different localized traps for hydrogen molecules which are identified from the dependence on the ion dose and annealing behavior. Each of these traps, which is saturated with H_2, gives rise to three Raman transitions due to para- and ortho-H_2. The H_2 signals are shown to correlate with the Si-H vibrational modes at 1888, 1930, and 1964 cm^{-1}. Ortho to para conversion rates of H_2 at 77 K and room temperature were found to be 62 ± 15 and 8 ± 2 h, respectively.

DOI: 10.1103/PhysRevB.86.125205 PACS number(s): 78.30.Am, 61.72.jd, 61.72.uf, 61.80.Jh

I. INTRODUCTION

Molecular hydrogen in silicon may occur at various places of the host lattice: (i) the interstitial T_d site[1,2]; (ii) in hydrogen-induced platelets[3]; (iii) bound to interstitial oxygen[4–7]; or (iv) trapped in multivacancies.[8,9]

Implantation of high energy ions results in the formation of different intrinsic defects, among others vacancy-related complexes. Raman spectra from samples subjected to a subsequent hydrogenation reveal a vibrational band of hydrogen molecules at 3820 cm^{-1}.[8,9] The same signal also appears in the spectra of proton-implanted silicon[10]—a key part of the ion-cut technology developed to transfer and bond thin Si layers to a silicon substrate.[11]

It has been always assumed that the blistering of the surface layer in the ion-cut wafer occurs due to the pressurized H_2 gas filling the blister cavities.[12] Thus, it seems to be natural to suggest that the 3820-cm^{-1} band is due to molecules trapped in multivacancies which serve as precursors for the cavities.[8,9] The 3820-cm^{-1} band, however, disappears from the Raman spectra after annealing the samples at around 250 °C, which indicates that it cannot be directly related to H_2 pressurizing the blisters that show up at higher temperatures.

The isolated vacancy and a number of complexes containing vacancies have been observed experimentally and discussed theoretically.[13] Theory predicts that the ring hexavacancy (V_6) is a particularly stable defect[14,15] which in photoluminescence (PL) gives rise to the J lines (B^4_{80} center).[16–18] Hourahine *et al.* have found that if the material contains hydrogen molecules, these will be readily trapped by V_6 where H_2 dissociates with a barrier of less than 0.23 eV and forms Si-H complexes,[16] giving rise to the trigonal V_6H_2 defects associated with the B_{41} and B^1_{71} PL centers.[19,20]

Saito *et al.*[21] and Akiyama and Oshiyama[22] theoretically investigated H_2 trapped in hydrogen saturated vacancies VH_4, V_2H_6, V_6, and V_{10}. The vibrational modes of the molecules were found to be between those of the gas phase (4161 cm^{-1}) and that of the interstitial T_d site (3627 cm^{-1}). The frequency of H_2 grows with the cluster size and reaches the vacuum value already for V_6H_{12}. The authors suggested that the 3820-cm^{-1} band is associated with H_2 at V_2H_6. No unambiguous experimental evidence, however, has been presented that hydrogen molecules exist in multivacancies.

Here we report the results of a combined Raman scattering and photoluminescence study performed at liquid helium temperatures. Single crystalline silicon samples were implanted with ^{28}Si ions and subsequently hydrogenated from an rf plasma at 200 °C. Earlier Raman investigations, carried out at room temperature, could not unveil the nature of the 3820-cm^{-1} band, in particular, due to significant broadening of this vibrational mode.[8–10,23]

The total nuclear spin of H_2 can be either 1 (ortho hydrogen, o-H_2) or 0 (para hydrogen, p-H_2). According to the Pauli principle the total wave function of any fermionic system has to be antisymmetric with respect to the permutation of the nuclei. Hence, only odd (even) values of the rotational quantum number J are allowed for o-H_2 (p-H_2).[24] The conversion between p- and o-H_2 in silicon is remarkably slow because the nuclear spin of proton interacts only weakly with the lattice. Ortho-para conversion for interstitial H_2,[25,26] the molecule bound to oxygen,[27] and in hydrogen-induced platelets[28] was investigated. The origin of a magnetic moment resulting in the nuclear spin flip of H_2 is still not clear though a number of models were discussed.[25,26,29] Here the conversion rate of H_2 giving rise to the 3820-cm^{-1} band is studied to get further insight into the defect's structure.

II. EXPERIMENTAL DETAILS

For this study, p-type float-zone silicon wafers with a resistivity of 9.5 Ω cm were implanted with 200 keV ^{28}Si ions to the doses of 8×10^{13}, 2×10^{14}, and 4×10^{14} cm^{-2}, respectively. According to SRIM simulations,[30] the penetration depth of Si ions at this energy is 450 nm. Subsequently, the samples were hydrogenated from a remote rf plasma (13.56 MHz, 40 W) at 200 or 230 °C for 30 min.

Raman measurements were performed using the 532 nm Nd:YVO_4 laser line (1 W) for excitation. The samples were mounted in a coldfinger cryostat cooled with liquid He. The temperature of the sample during the measurements was controlled from the Stokes/anti-Stokes intensity ratio of the silicon optical phonon line at 520 cm^{-1} and reached around 60 K. The spectral resolution was 7 cm^{-1}, whereas the integration time varied between 1 and 4 h. Polarized Raman spectra were measured at room temperature. The polarization

geometry is defined with respect to the (100) surface of the sample: The x, y, and z axis are parallel to the crystallographic axis [100], [010], and [001], whereas y' and z' are parallel to $[01\bar{1}]$ and [011], respectively. In the notation $[a(b,c)d]$, $a(d)$ refers to the propagation vector of the incident (scattered) light, while $b(c)$ refers to the polarization vector of the incident (scattered) light. The polarized spectra were corrected with respect to the grating efficiency by calibration with a white light source.

Photoluminescence spectra were obtained with a 514 nm Ar^+ laser (50 mW). During the measurements, the samples were immersed in a helium bath cryostat.

III. RAMAN AND PHOTOLUMINESCENCE SPECTRA

A. General properties of the Raman lines

Figure 1 presents Raman spectra obtained for silicon samples implanted with ^{28}Si ions and subsequently hydrogenated from an rf plasma. The left panel in the figure shows the optical lattice phonon signal at 520 cm^{-1}. Its intensity decreases with the implantation dose, which is explained by the enhanced radiation damage of the sample caused by the ^{28}Si ions.

The panel in the middle of the figure shows sections of the Raman spectra typical for the Si-H local vibrational modes (LVMs). The lines at 2148, 2190, and 2220 cm^{-1} originate from the vacancy-hydrogen complexes VH_2, V_2H_6, and VH_4, respectively.[31,32] Two weak features at 2025 and 2043 cm^{-1} were previously assigned to the LVMs of some unknown hydrogen-terminated Si dangling bonds.[23] The 1964-cm^{-1} line was tentatively attributed to hydrogen saturated multivacancies.[8] The nature of the 1888- and 1930-cm^{-1} lines is unknown.

The right panel in the figure presents LVMs of H_2 at around 3830 cm^{-1}. Similar to the 520-cm^{-1} phonon line, the integrated intensity of this band decreases with the implantation dose. The 3830-cm^{-1} feature reveals a substructure, which, due to the thermal broadening of the Raman signals at elevated temperatures, can be detected only for temperatures

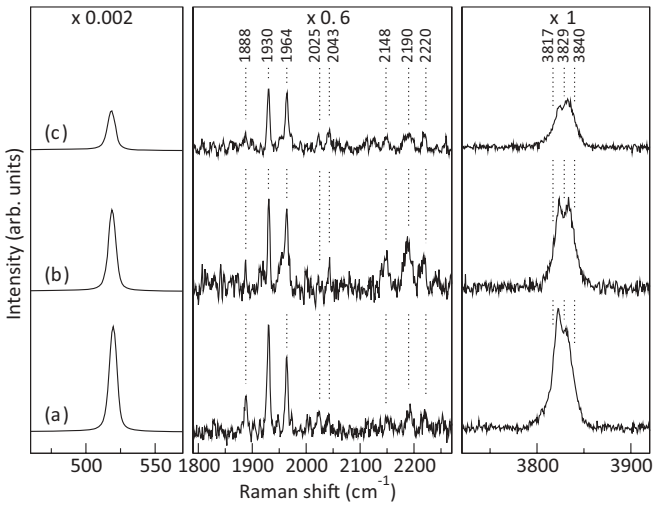

FIG. 1. Raman spectra of an as-prepared Si sample obtained at 60 K. The Si ion implantation doses are (a) 8×10^{13}, (b) 2×10^{14}, and (c) 4×10^{14} cm^{-2}. The spectra are vertically offset for clarity.

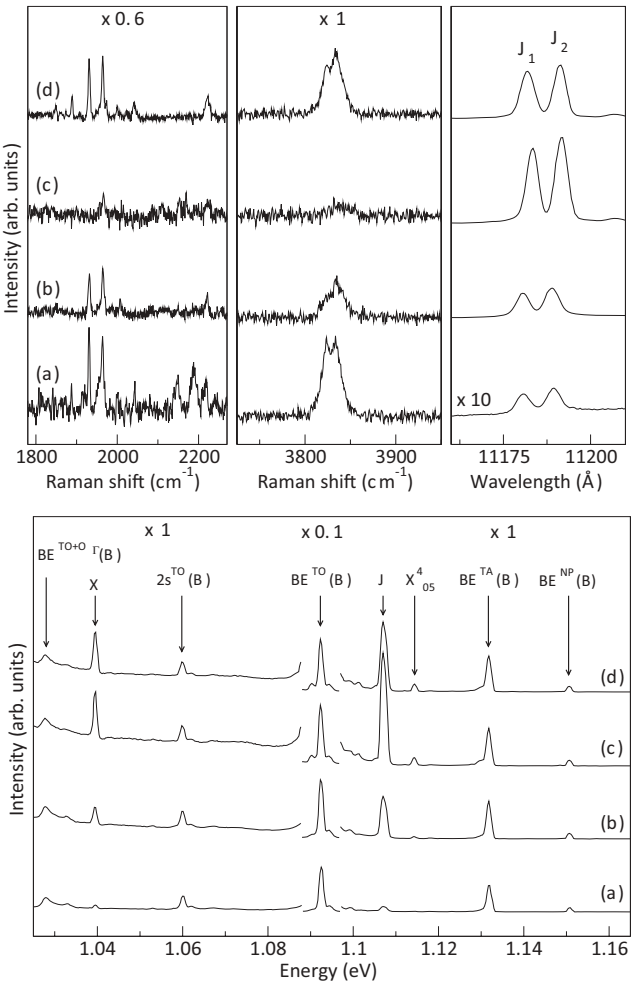

FIG. 2. Top: Raman (left and mid) and PL (right) spectra recorded for (a) an as-prepared Si sample; (b) after annealing at 250 and (c) 300 °C; and (d) after subsequent rehydrogenation at 200 °C. The Raman and PL measurements were performed at 60 and 4.2 K, respectively. The Si ion implantation dose is 2×10^{14} cm^{-2}. The spectra are vertically offset for clarity. Bottom: PL spectra of the whole spectral range taken under same conditions like the upper spectra.

below 100 K. The shape of the 3830-cm^{-1} band also depends on the implantation dose, which suggests that there are at least two different binding centers for the molecule. We will show in the next section that this band is composed of three complexes containing hydrogen molecules which give rise to $Q(0)$ transitions at 3840, 3829, and 3817 cm^{-1}. We will label these complexes as $K^{(1)}$, $K^{(2)}$, and $K^{(3)}$, respectively.

Ishioka *et al.* associated the 3830-cm^{-1} band with H_2 trapped in multivacancies formed by the ion implantation.[9] In order to get a deeper insight into the nature of the $K^{(1)}$, $K^{(2)}$, and $K^{(3)}$ complexes, an annealing series up to 300 °C followed by a rehydrogenation was performed. After each processing step, Raman and photoluminescence spectra were obtained. The results are presented in Fig. 2.

In accordance with previous studies, we find that the VH_2 and V_2H_6 complexes are unstable against annealing at 300 °C, whereas VH_4 can be destroyed only at temperatures above 500 °C.[31,32] The results presented in the figure are

also consistent with the assignment of the 3817-, 3829-, and 3840-cm^{-1} modes of H_2 to different complexes since the relative intensities of these lines depend on the details of the sample treatment. We also conclude that the $K^{(1)}$ complex is thermally more stable than $K^{(2)}$ and $K^{(3)}$.

The H_2 vibrational modes practically disappear from the spectra after annealing at 300 °C together with the LVMs of Si-H at 1888, 1930, and 1964 cm^{-1}. Interestingly, these signals are recovered after an additional hydrogenation at 200 °C, which suggests that the binding centers for hydrogen are stable up to 300 °C.

As mentioned above, hydrogen-saturated hexavacancies were discussed as possible traps for H_2 giving rise to the 3830-cm^{-1} band. Previously, it was shown that the photoluminescence signal at around 1.107 eV (J lines or B_{80}^4 centers)[17,18,33] originates from V_6.[16] In order to find out if there is a connection between the 3830-cm^{-1} band and the J lines, PL spectra were recorded after each annealing step and an additional rehydrogenation (right panel in upper spectrum of Fig. 2). The photoluminescence spectra of the whole spectral range (bottom of Fig. 2) show mostly boron-related excitonic signals. Three radiation-induced peaks at 1.0398 eV (X center[34]), 1.1075 eV (J lines or B_{80}^4 center), and 1.1144 eV (X_{05}^4 center[35]) are present in all spectra and show similar annealing behavior. It is expected that the intensities of the J lines after rehydrogenation [Fig. 2(d), top spectra] are close to those (a factor of 30 weaker) obtained for the as-prepared samples [Fig. 2(a), top spectra] if the 3830-cm^{-1} line originates from the V_6H_2 complex. However, no unambiguous anticorrelation between V_6 and the 3830 cm^{-1} is seen, which leads us to the conclusion that the hexavacancy is not responsible for the 3830-cm^{-1} band.

It follows from Fig. 2 that only Si-H modes at 1888, 1930, and 1964 cm^{-1} seem to correlate with the 3830-cm^{-1} band. First-principles calculations by Akiyama and Oshiyama have found that of all hydrogen-saturated vacancies V_nH_m only the V_6H_{12} complex and those with $n > 6$ reveal Si-H modes in the spectroscopic region below 2000 cm^{-1}.[22] On the other hand, vibrational frequencies of H_2 trapped in these structures are close to that of the gaseous state (4161 cm^{-1}). Therefore it seems unlikely that V_nH_m complexes can trap H_2 resulting in the 3830 cm^{-1} band.

B. ISOTOPE SUBSTITUTION

Figure 3 presents Raman spectra taken after ion implantation at a dose of 8×10^{13} cm^{-2} and subsequent rf-plasma treatment with hydrogen, deuterium, and a mixture of both gases, respectively. The modes at 1888, 1930, and 1964 cm^{-1} redshift to 1375, 1405, and 1430 cm^{-1} after substitution of hydrogen by deuterium. Note that the broad band at 1450 cm^{-1} originates from the second overtone of the silicon lattice phonon. No additional lines appear in the spectra if a sample is treated simultaneously with both isotopes. Such a behavior indicates that each defect responsible for these modes comprises a single Si-H bond. A substructure of the hydrogen modes at 1888, 1930, and 1964 cm^{-1} cannot be resolved in our spectra due to the maximum resolution of our Raman setup which is 3 cm^{-1}.

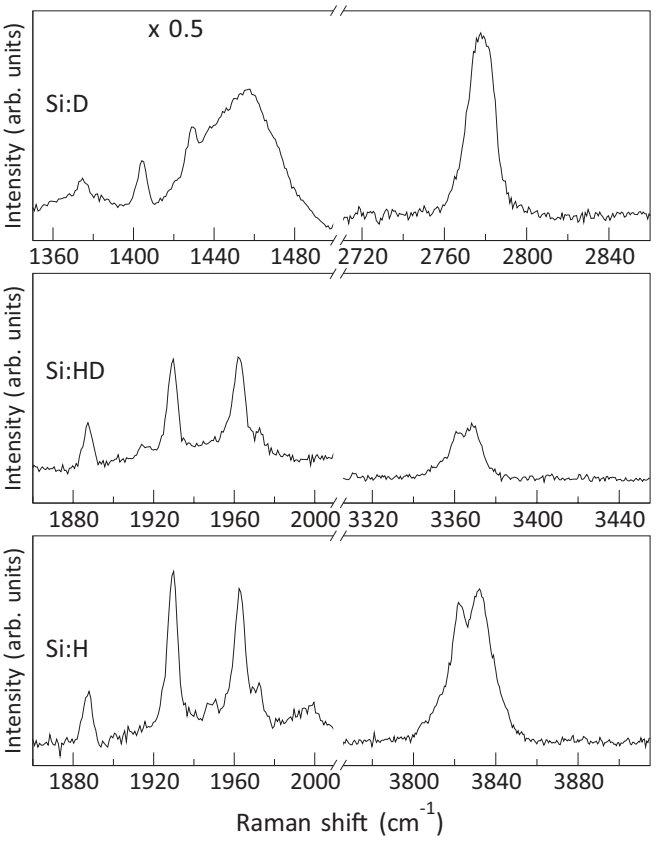

FIG. 3. Raman spectra of Si samples treated in a H_2 (bottom), $H_2 + D_2$ (middle), and D_2 plasma (top) at 230 °C, respectively, after ion implantation with a dose of 8×10^{13} cm^{-2}.

Isotope substitution experiments reveal the correlation between the 1888-, 1930-, and 1964-cm^{-1} modes and the 3817-, 3829-, and 3840-cm^{-1} lines comprising the 3830-cm^{-1} band. We will show below that it takes days to convert ortho molecules to the ground para state at 77 K. This implies that each H_2 Raman signal taken at helium temperatures consists of at least two lines due to the ortho and para species. Altogether, this should result in six lines comprising the 3830-cm^{-1} band, which significantly complicates an analysis of the experimental data. The line shape of the D_2 band at 2780 cm^{-1} differs from that one of the 3830-cm^{-1} band. The absence of a splitting is explained with the smaller ortho-para splitting of D_2 (~3 cm^{-1}) in comparison to H_2 (~9 cm^{-1}) which follows from the Morse potential.[36] This makes the quantitative analysis of the D_2 LVMs even more difficult.

The situation is different for HD where all J states are in thermal equilibrium. At helium temperatures only the ground $J = 0$ state of HD is populated. Figure 4 shows Raman spectra of a Si sample implanted with Si ions to the dose of 8×10^{13} cm^{-2} and subsequently treated in the $H_2 + D_2$ plasma at 230 °C. The spectra were taken directly after the treatment and after annealing at 240 °C. Relative intensities of the Si-H modes at 1888, 1930, and 1964 cm^{-1} depend on the sample history and are 17:35:48 and 6:35:58 for the as-treated and annealed sample, respectively.

Spectra of the HD band at about 3360 cm^{-1} are given in the right panel of the figure. The 3360-cm^{-1} band was

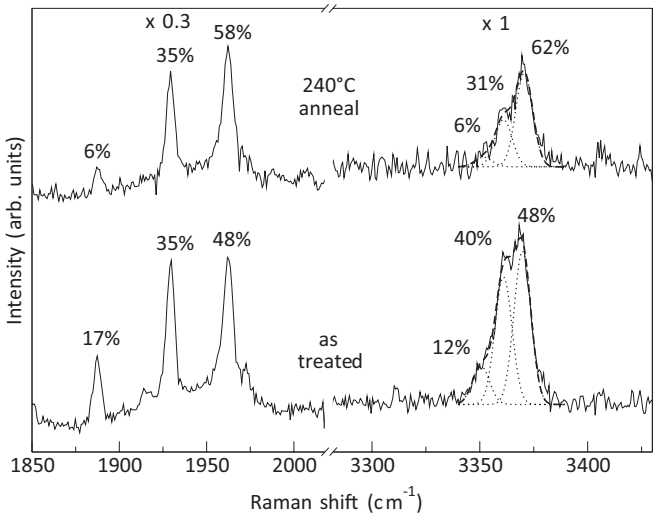

FIG. 4. Raman spectra of a Si sample treated in a $H_2 + D_2$ plasma at 230 °C (bottom) and after subsequent annealing at 240 °C (top) obtained at 60 K. The Si ion implantation dose was 8×10^{13} cm^{-2}. For details of the fit (dashed lines) see text. The integrated intensities of the peaks normalized on the entire Si-H and HD intensities, respectively, are also given. Spectra are offset vertically for clarity.

fitted with three Gaussian functions of equal linewidth (dashed lines). Relative intensities of the fitting lines at 3351, 3360, and 3370 cm^{-1} were found to be 12:40:48 and 6:31:62 for the as-treated and annealed sample, respectively. This coincides within error bars with the relative intensities of the Si-H modes and gives us further support for the same origin of the 1888-, 1930-, and 1964-cm^{-1} lines and those comprising the 3830-cm^{-1} band.

C. Thermal stability

Figure 5 presents relative intensities of the Si-H and H_2 modes as a function of the annealing temperature. In agreement with the results presented in Figs. 1, 2, and 4 the intensities of the 1888-, 1930-, and 1964-cm^{-1} lines correlate with those of the K complexes, which confirms the same origin of the LVMs due to Si-H and H_2. It also follows from the figure that thermal stability of the species grows in with the LVM frequency of the complex: The $K^{(1)}$ complex is detected at about 290 °C, whereas $K^{(3)}$ disappears from the spectra after anneal at about 260 °C.

Our results are supported by the work of Mori *et al.* who found that the 3820-cm^{-1} band (RT value) consists of two lines with different thermal stabilities.[37] In this study, the low frequency line anneals out at 200 °C, whereas the high frequency one disappears from the spectra after anneal at 240 °C. The quantitative difference between our results and those reported by Mori *et al.* can be explained by different experimental conditions (starting material, implantation doses, parameters of hydrogenation, etc.).

D. Polarized Raman spectra

Figure 6 presents polarized Raman spectra obtained at room temperature in four different scattering geometries labeled in the left panel of the figure. The sample was hydrogenated at

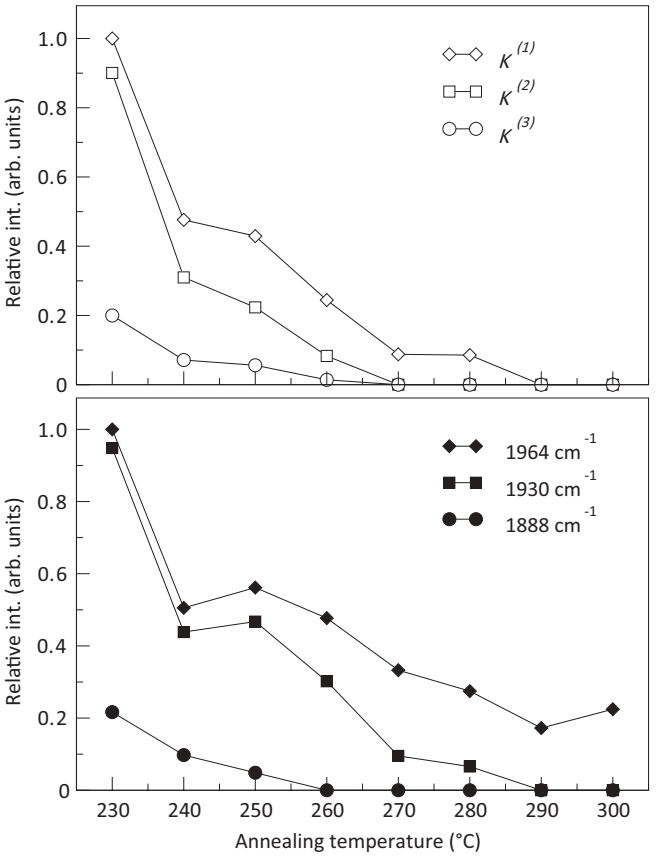

FIG. 5. Relative intensities of the H_2 and Si-H LVMs taken at 60 K after as a function of annealing temperature. The implantation dose was 8×10^{13} cm^{-2}. Hydrogenation was done at 230 °C.

230 °C. The H_2 band is polarized with the excitation laser light independent of the measurement geometry. This is a typical behavior of interstitial H_2 in Si which follows from the values of its Raman tensor resulting in the reduction of

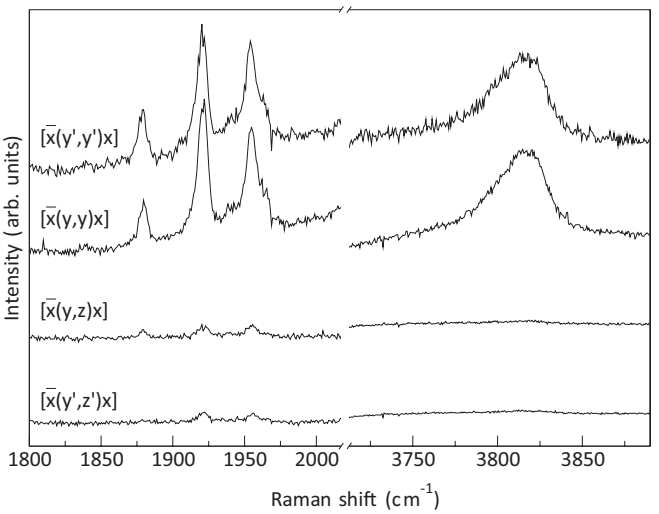

FIG. 6. Polarized Raman spectra of an as-treated sample taken at room temperature. For details of the geometry see Sec. II. Spectra are offset vertically for clarity.

the components obtained for the $[\bar{x}(y',z')x]$ and $[\bar{x}(y,z)x]$ geometries by around a factor of 50.[7,38]

The left panel in the figure shows the polarized Raman spectra of the Si-H modes at 1880, 1922, and 1956 cm^{-1}. Note the redshift of these lines due to the temperature of about 300 K during the polarization dependent measurements. The 1880-cm^{-1} line is most intense in the $[\bar{x}(y',y')x]$ geometry and is basically zero in the $[\bar{x}(y',z')x]$ geometry. This is a typical behavior of a defect with a trigonal symmetry (see Ref. 32) based on which the 1880-cm^{-1} mode can be associated with a Si-H bond aligned in the $\langle 111 \rangle$ direction of the crystal.

The polarization behavior of the 1922- and 1956-cm^{-1} modes is different from that of the 1880-cm^{-1} one. Both lines have maximum intensities in the $[\bar{x}(y',y')x]$ and $[\bar{x}(y,y)x]$ geometries, which are reduced by more than 90% in the $[\bar{x}(y',z')x]$ and $[\bar{x}(y,z)x]$ geometries. None of the lines disappear in the case of $[\bar{x}(y',z')x]$ orientation, which indicates that the Si-H bonds comprising the defects are not aligned with the $\langle 111 \rangle$ axis of the crystal. We take this as further indication that the defect complexes responsible for the 1922- and 1956-cm^{-1} lines cannot be associated with the multivacancies saturated by hydrogen. Earlier, it was shown that Si-H bonds in such centers are basically aligned with the trigonal axes of the crystal.[32]

IV. QUANTITATIVE MODEL

Regardless of the nature of the $K^{(1)}$, $K^{(2)}$, and $K^{(3)}$ complexes, the vibrational spectrum of H_2 at low temperatures should consist of transitions due to p- and o-H_2 in the $J = 0$ and 1 states, respectively. In the next subsection we will show that at low temperatures the ortho-para conversion rate of H_2 giving rise to the 3830-cm^{-1} band is significantly slower compared to the measurement time. This implies that the ortho-to-para ratio in the spectra presented in Fig. 1 is equal to the room temperature value of 3:1.

The rotational J states of H_2 are given by[24]

$$E(v,J) = B_v J(J+1), \tag{1}$$

where

$$B_v = \frac{\hbar^2}{2\mu r_0^2} - \alpha_e \left(v + \frac{1}{2}\right). \tag{2}$$

Here v is the vibrational quantum number, μ is the reduced mass of H_2, and r_0 is the equilibrium distance between the hydrogen atoms in the molecule. Energetic and vibrational frequencies of H_2 in different semiconductors were considered theoretically in Ref. 39. The force constant was found to be a linear function of r_0. From there we obtain that the interatomic distance for H_2 giving rise to the 3830-cm^{-1} band is 0.77 Å, which is between the values found for interstitial H_2 in Si (0.788 Å) and that of the free molecule (0.751 Å).[40,41]

Assuming that H_2 is trapped by a spherically symmetric potential, each K complex would result in two lines due to the $Q(1)$ and $Q(0)$ transitions with the relative intensities of 3:1, respectively. The frequency difference between the $Q(1)$ and $Q(0)$ modes is determined by the anharmonic part of the vibrational potential α_e [see Eq. (2)], which, in turn, can be estimated from the frequency of the D_2 counterpart of the 3830-cm^{-1} band. Employing the Morse function to model the vibrational potential[24,42] we get that each of the K signals should comprise a pair of lines split by about 8 cm^{-1} with relative intensities of 3:1.

The model of freely rotating H_2, however, does not result in a reasonable fit of the 3830-cm^{-1} band. This leads us to the conclusion that the threefold degeneracy of the $J = 1$ state is lifted by the binding potential. Similar situation takes place for H_2 bound to interstitial oxygen in Si where the $Q(1)$ transition of o-H_2 splits into two states corresponding to the $m = \pm 1$ and 0 projections of the angular momentum.[6,7]

In order to analyze the structure of the 3830-cm^{-1} band quantitatively, we employ the simplest binding potential, whose spherical part with the z axis passing through the trap and the center of H_2 is given by (a more sophisticated treatment can be found in Ref. 43)

$$V(\theta) = V_0 \cos^2\theta. \tag{3}$$

The eigenvalues of the perturbed system are found by diagonalization of the corresponding Hamiltonian matrix $\langle Y_J^{m_J}|V(\theta)|Y_L^{m_L}\rangle$. Here the spherical harmonics $Y_J^{m_J}$ form the basis set of the unperturbed system. Altogether, the 3830-cm^{-1} band should comprise three groups of the $Q(0)$, $Q_0(1)$, and $Q_{\pm 1}(1)$ lines each of which is due to the $K^{(1)}$, $K^{(2)}$, and $K^{(3)}$ complexes. Note that the intensity ratio of the $Q_0(1)$ and $Q_{\pm 1}(1)$ transitions is now a function of temperature proportional to the Boltzmann factor $\exp(-\Delta E/kT)$, where ΔE is the energy difference between the $m = \pm 1$ and 0 states of o-H_2.

Figure 7 presents a spectrum of the 3830-cm^{-1} band recorded at 60 K together with the best-fit spectrum obtained according to the procedure described above. Note that only six fitting parameters were employed to simulate this spectrum. These are the value of the perturbation potential V_0, the relative concentrations of the $K^{(1)}$, $K^{(2)}$, and $K^{(3)}$ complexes, and the frequencies of the $Q(0)$ modes. As seen from the figure, the simulated spectrum can adequately account for the shape of the

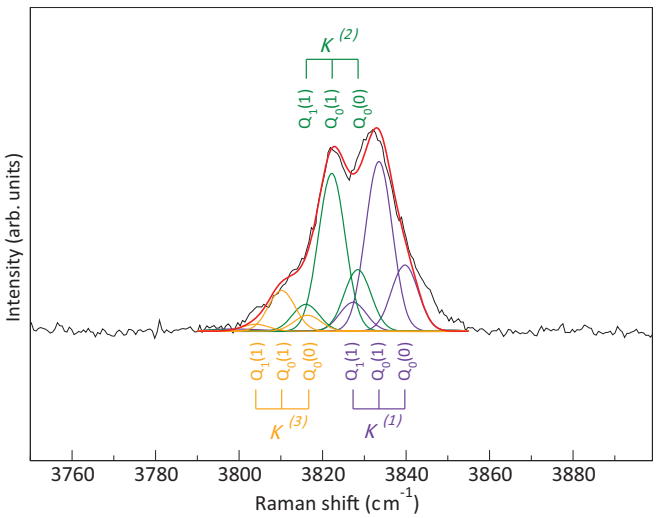

FIG. 7. (Color online) Experimental (black) and simulated (red) Raman spectra of H_2 in the K defects. The experimental spectrum was obtained at 60 K for an as-prepared Si sample. The implantation dose was 8×10^{13} cm^{-2}; the temperature during hydrogenation was 230 °C. The ortho/para ratio is 3:1. For details of the fit see text.

TABLE I. Intensity ratios of the H_2 signals comprising the 3830 cm^{-1} band ($K^{(2)}/K^{(1)}$ and $K^{(3)}/K^{(1)}$) and the Si-H modes at 1888, 1930, and 1964 cm^{-1} as a function of the implantation dose.

Dose (cm^{-2})	$K^{(2)}/K^{(1)}$	I_{1930}/I_{1964}	$K^{(3)}/K^{(1)}$	I_{1888}/I_{1964}
8×10^{13}	1.44	1.17	0.28	0.27
2×10^{14}	1.06	0.92	0.20	0.17
4×10^{14}	0.94	0.91	0.26	0.26

TABLE II. Ortho-para conversion rates (h) of H_2 trapped at different sites of Si lattice determined at 77 and 300 K.

Trap	77 K	300 K	Ref.
T_d interstitial	229 ± 14	8.1 ± 0.5	26
O_i	140 ± 50	–	27
{111} platelets	9 ± 4	6 ± 4	28
K complexes	62 ± 15	8 ± 2	this work

3830-cm^{-1} band. The fit was also successfully employed to all those spectra recorded at different temperatures, for different implantation doses, and ortho-to-para ratios.

The simulations performed for different samples lead us to the energy-level diagrams of H_2 in the K complexes presented in Fig. 8. Note that the $J = 1$ state is split by 88 cm^{-1}, which is comparable to the value of 60 cm^{-1} found for hydrogen bound to the interstitial oxygen in Si.[6,7]

The relative occurrences of the three H_2 signals comprising the 3830-cm^{-1} band, $K^{(2)}/K^{(1)}$ and $K^{(3)}/K^{(1)}$, determined from the simulated spectra are listed in Table I together with the intensity ratios I_{1930}/I_{1964} and I_{1888}/I_{1964} of the Si-H LVMs at 1888, 1930, and 1964 cm^{-1}. As pointed out before, the K complexes correlate with the 1888-, 1930-, and 1964-cm^{-1} lines.

Known hydrogen-related defects with frequencies of the Si-H vibrational modes below 2000 cm^{-1} are the hydrogen saturated self-interstitial IH_2 (1989.4, 1986.5, 748.0, and 743.1 cm^{-1}) and the hydrogen dimer H_2^* (2061.5, 1838.3, 1599.1, and 817.2 cm^{-1}).[44,45] The H_2^* dimer consists of one hydrogen atom located at the bond-centered site, whereas the second one occupies the antibonding position of the Si lattice. It is unlikely that the H_2^* complex acts as a binding center for hydrogen molecules, because it anneals out at 200 °C.[44] This is in contradiction to the annealing behavior shown in Fig. 2, where the Si-H and H_2 LVMs are recovered after annealing at 300 °C and an additional hydrogenation. The IH_2 defect, which originates from an intrinsic point defect, seems to be a more reasonable candidate for a binding center of hydrogen molecules. We speculate, therefore, that the 3830-cm^{-1} band is associated with the molecule trapped at interstitial-like defects rather than multivacancies. LVMs of the trapping centers deviate from the unperturbed values due to the interaction with the nearby H_2. Note that similar situation takes place in the case of the molecule trapped at the interstitial oxygen, where the LVM of oxygen in the presence of H_2 shifts downwards in frequency to 1075 cm^{-1} from the unperturbed value of 1136 cm^{-1}.[4] We emphasize, however, that our suggestion about the nature of the trapping centers for hydrogen needs support from theoretical calculations.

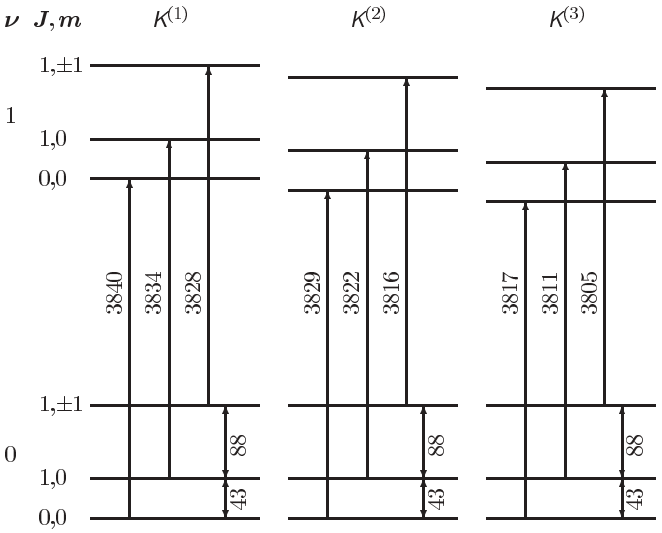

FIG. 8. Energy-level diagram of the first three rovibrational transitions of H_2 in $K^{(1)}$, $K^{(2)}$, and $K^{(3)}$. All values are given in cm^{-1}.

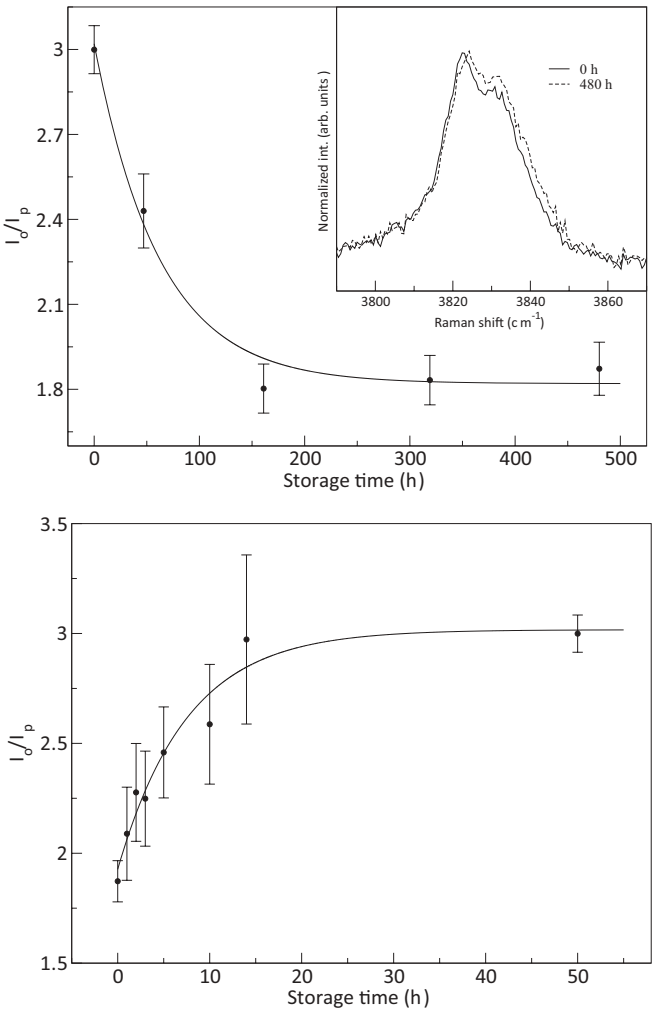

FIG. 9. Ortho-to-para ratio (I_o/I_p) as a function of storage time at 77 (top) and 300 K (bottom). Solid lines—exponential fit with the conversion rates of 62 and 8 h, respectively. The inset shows the normalized Raman spectra obtained at 0 and 480 h.

V. ORTHO-PARA CONVERSION

Energy-level diagrams of H_2 in the K complexes presented in Fig. 8 allow us to probe the ortho-para conversion rate. Because the rovibrational properties of the hydrogen molecules in the three defects seem to be very similar, we assume that the conversion dynamic is almost the same.

Rotational levels of H_2 with $J > 1$ are practically not populated at the temperatures employed in our study and can be disregarded. Because of this, the equlibrium ortho-para ratio is determined by the lowest three levels of the molecule

$$\frac{I_o}{I_p} = 3\frac{e^{-E_0(1)/kT} + 2e^{-E_{\pm1}(1)/kT}}{e^{-E(0)/kT}}. \quad (4)$$

Here $E_m(J)$ is the energy of the rotational state with a total angular momentum J and its projection m. The prefactor 3 comes from the different nuclear spin state degeneracies of the two hydrogen species. From Eq. (4) and the energy-level diagram presented in Fig. 8 we obtain that at 77 K the ortho-para ratio should be 1.8:1, which significantly differs from the cases of free and interstitial H_2 resulting in equal number of each species ($I_o/I_p = 1$).[25]

In order to determine the ortho-para conversion rate at 77 K, the samples were stored in LN_2 for nearly 500 h. During the storage Raman measurements at 60 K were performed and the spectra were analyzed according to the procedure described in the previous subsection. The results are presented in Fig. 9. The solid line is the best-fit curve to the experimental data under assumption of a single exponential decay. As follows from the figure, the equilibrium value of $I_o/I_p \approx 1.8$ agrees with the one estimated above from Eq. (4) on the basis of the energy-level diagram of H_2. From the fitting procedure we obtain that the ortho-para conversion rate is 62 ± 15 h.

The ortho-para conversion at 300 K (see bottom panel of Fig. 9) was also investigated. As expected, the back conversion is a faster process yielding the rate of 8 ± 2 h.

These values should be compared to those obtained for interstitial molecules,[25,26] H_2 bound to the interstitial oxygen,[27] and hydrogen trapped in platelets,[28] which are gathered in Table II. We see that the conversion rate of H_2 bound to the K complexes is between the value found for interstitial molecule and those trapped in the $\{111\}$ platelets. The latter system represents a two-dimensional gas under high pressure, so that the main mechanism resulting in nuclear spin flip is expected to be interaction between the neighboring molecules.[28]

The ortho-para conversion mechanism for interstitial H_2 is still not clear.[25,26,29] The conversion rate of H_2 giving rise to the 3830-cm^{-1} band indicates that the nature of the nuclear spin flip is closer to that of interstitial molecules and molecules bound to interstitial oxygen rather than those trapped in platelets.

VI. SUMMARY

Raman and photoluminescence spectra of ^{28}Si-ion implanted and subsequently hydrogenated single crystalline silicon were presented. Such samples reveal a broad Raman line at 3830 cm^{-1} (60 K) due to the rovibrational transitions of H_2. The 3830-cm^{-1} band reveals a complex structure, which is assigned to three different traps for hydrogen occurring in concentrations which depend on the sample history. The H_2 signals comprising the band are shown to correlate with the Si-H vibrational modes at 1888, 1930, and 1964 cm^{-1}. Based on this correlation it is concluded that multivacancies cannot be the trapping centers for H_2. Ortho to para conversion rates of H_2 at 77 and 300 K found to be 62 ± 15 and 8 ± 2 h, respectively.

ACKNOWLEDGMENTS

This work was supported by the Deutsche Forschungsgemeinschaft (Grant No. LA 1397/3-1). S. Eisenwinder (Helmholtz-Zentrum Dresden-Rossendorf) is acknowledged for performing the ion implantation of our samples. The authors thank M. Allardt for the help with the photoluminescence measurements.

*sebastian.socher@physik.tu-dresden.de

[1] R. E. Pritchard, M. J. Ashwin, J. H. Tucker, and R. C. Newman, Phys. Rev. B **57**, R15048 (1998).
[2] A. W. R. Leitch, V. Alex, and J. Weber, Phys. Rev. Lett. **81**, 421 (1998).
[3] E. V. Lavrov and J. Weber, Phys. Rev. Lett. **87**, 185502 (2001).
[4] R. E. Pritchard, M. J. Ashwin, J. H. Tucker, R. C. Newman, E. C. Lightowlers, M. J. Binns, S. A. McQuaid, and R. Falster, Phys. Rev. B **56**, 13118 (1997).
[5] V. P. Markevich and M. Suezawa, J. Appl. Phys. **83**, 2988 (1998).
[6] E. E. Chen, M. Stavola, and W. B. Fowler, Phys. Rev. B **65**, 245208 (2002).
[7] M. Hiller, E. V. Lavrov, and J. Weber, Phys. Rev. B **74**, 235214 (2006).
[8] K. Murakami, K. Ishioka, M. Kitajima, S. Tateishi, K. Nakanoya, T. Mori, and S. Hishita, Physica B **273-274**, 188 (1999).
[9] K. Ishioka, M. Kitajima, S. Tateishi, K. Nakanoya, N. Fukata, T. Mori, K. Murakami, and S. Hishita, Phys. Rev. B **60**, 10852 (1999).
[10] J. Weber, T. Fischer, E. Hieckmann, M. Hiller, and E. V. Lavrov, J. Phys.: Condens. Matter **17**, S2303 (2005).
[11] M. Bruel, Electron. Lett. **31**, 1201 (1995).
[12] M. K. Weldon, V. E. Marsico, Y. J. Chabal, A. Agarwal, D. J. Eaglesham, J. Sapjeta, W. L. Brown, D. C. Jacobson, Y. Caudano, S. B. Christman, and E. E. Chaban, *The 24th Conference on the Physics and Chemistry of Semiconductor Interfaces* (American Institute of Physics, Woodbury, NY, 1997), Vol. 15, p. 1065.
[13] G. D. Watkins, in *Deep Centers in Semiconductors*, edited by S. T. Pantelides (Gordon and Breach, New York, 1986).
[14] J. L. Hastings, S. K. Estreicher, and P. A. Fedders, Phys. Rev. B **56**, 10215 (1997).
[15] D. J. Chadi and K. J. Chang, Phys. Rev. B **38**, 1523 (1988).
[16] B. Hourahine, R. Jones, A. N. Safonov, S. Öberg, P. R. Briddon, and S. K. Estreicher, Phys. Rev. B **61**, 12594 (2000).
[17] R. Sauer and J. Weber, Physica B + C **116**, 195 (1983).
[18] A. S. Kaminskii and E. V. Lavrov, Solid State Commun. **106**, 751 (1998).
[19] A. S. Kaminskii, E. V. Lavrov, V. A. Karasyuk, and M. L. W. Thewalt, Phys. Rev. B **50**, 7338 (1994).

[20]A. S. Kaminskii, E. V. Lavrov, V. A. Karasyuk, and M. L. W. Thewalt, Solid State Commun. **97**, 137 (1996).
[21]M. Saito, Y. Okamoto, A. Oshiyama, and T. Akiyama, Physica B **273-274**, 196 (1999).
[22]T. Akiyama and A. Oshiyama, Physica B **273-274**, 516 (1999).
[23]T. Mori, K. Otsuka, N. Umehara, K. Ishioka, M. Kitajima, S. Hishita, and K. Murakami, Physica B **308-310**, 171 (2001).
[24]L. D. Landau and E. M. Lifschitz, *Quantum Mechanics: Non-Relativistic Theory*, 3rd ed. (Pergamon Press, Oxford, England, 1977).
[25]M. Hiller, E. V. Lavrov, and J. Weber, Phys. Rev. Lett. **98**, 055504 (2007).
[26]C. Peng, M. Stavola, W. B. Fowler, and M. Lockwood, Phys. Rev. B **80**, 125207 (2009).
[27]M. Hiller, E. V. Lavrov, and J. Weber, Physica B **401-402**, 97 (2007).
[28]M. Hiller, E. V. Lavrov, and J. Weber, Phys. Rev. B **80**, 045306 (2009).
[29]J. S. R. M. Herman, A. Suarez and J. C. Lewis, Proceedings of the 20th International Conference on Spectral Line Shapes **1290**, 284 (2010).
[30]J. F. Ziegler, M. Ziegler, and J. Biersack, Nucl. Instrum. Methods: Phys. Res. Sect. B **268**, 1818 (2010).
[31]B. B. Nielsen, L. Hoffmann, and M. Budde, Mater. Sci. Eng. B **36**, 259 (1996).
[32]E. V. Lavrov, J. Weber, L. Huang, and B. B. Nielsen, Phys. Rev. B **64**, 035204 (2001).
[33]E. S. Johnson and W. D. Compton, Radiat. Eff. **9**, 89 (1971).
[34]Z. Ciechanowska, G. Davies, and E. C. Lightowlers, Solid State Commun. **49**, 427 (1984).
[35]A. S. Kaminskii, A. N. Safonov, and E. V. Lavrov, Sov. Phys. Solid State **33(3)**, 488 (1991).
[36]E. V. Lavrov and J. Weber, Phys. Rev. Lett. **89**, 215501 (2002).
[37]T. Mori, K. Otsuka, N. Umehara, K. Ishioka, M. Kitajima, S. Hishita, and K. Murakami, Physica B **302-303**, 239 (2001).
[38]C. M. Hartwig and J. Vitko, Phys. Rev. B **18**, 3006 (1978).
[39]C. G. Van de Walle, Phys. Rev. Lett. **80**, 2177 (1998).
[40]E. E. Chen, M. Stavola, W. B. Fowler, and P. Walters, Phys. Rev. Lett. **88**, 105507 (2002).
[41]B. P. Stoicheff, Can. J. Phys. **35**, 730 (1957).
[42]G. Herzberg, *Molecular Spectra and Molecular Structure: I. Spectra of Diatomic Molecules* (Krieger, Malabar, FL, 1989).
[43]W. B. Fowler, P. Walters, and M. Stavola, Phys. Rev. B **66**, 075216 (2002).
[44]J. D. Holbech, B. Bech Nielsen, R. Jones, P. Sitch, and S. Öberg, Phys. Rev. Lett. **71**, 875 (1993).
[45]M. Budde, B. B. Nielsen, P. Leary, J. Goss, R. Jones, P. R. Briddon, S. Öberg, and S. J. Breuer, Phys. Rev. B **57**, 4397 (1998).